Cytoskeletal Architecture of Isolated Mitotic Spindle with Special Reference to Microtubule-associated Proteins and Cytoplasmic Dynein

NOBUTAKA HIROKAWA, REIKO TAKEMURA, and SHIN-ICHI HISANAGA
Department of Anatomy, School of Medicine, University of Tokyo, Hongo, Tokyo 113, Japan

ABSTRACT We have studied cytoskeletal architectures of isolated mitotic apparatus from sea urchin eggs using quick-freeze, deep-etch electron microscopy. This method revealed the existence of an extensive three-dimensional network of straight and branching crossbridges between spindle microtubules. The surface of the spindle microtubules was almost entirely covered with hexagonally packed, small, round button-like structures which were very uniform in shape and size (~8 nm in diameter), and these microtubule buttons frequently provided bases for crossbridges between adjacent microtubules. These structures were removed from the surface of microtubules by high salt (0.6 M NaCl) extraction. Microtubule-associated proteins (MAPs) and microtubules isolated from mitotic spindles which were mainly composed of a large amount of 75-kD protein and some high molecular mass (250 kD, 245 kD) proteins were polymerized in vitro and examined by quick-freeze, deep-etch electron microscopy. The surfaces of microtubules were entirely covered with the same hexagonally packed round buttons, the arrangement of which is intimately related to that of tubulin dimers. Short crossbridges and some longer crossbridges were also observed. High salt treatment (0.6 M NaCl) extracted both 75-kD protein and high molecular weight proteins and removed microtubule buttons and most of crossbridges from the surface of microtubules. Considering the relatively high amount of 75-kD protein among MAPs isolated from mitotic spindles, it is concluded that these microtubule buttons probably consist of 75-kD MAP and that some of the crossbridges in vivo could belong to MAPs.

Another kind of granule, larger in size (11–26 nm in diameter), was also on occasion associated with the surface of microtubules of mitotic spindles. A fine sidearm sometimes connected the larger granule to adjacent microtubules.

Localization of cytoplasmic dynein ATPase in the mitotic spindle was investigated by electron microscopic immunocytochemistry with a monoclonal antibody (D57) against sea urchin sperm flagellar 21S dynein and colloidal gold–labeled second antibody. Immunogold particles were closely associated with spindle microtubules. 76% of these were within 50 nm and 55% were within 20 nm from the surface of the microtubules. These gold particles were sporadically found on both polar and kinetochore microtubules of half-spindles at both metaphase and anaphase. They localized also on the microtubules between sister chromatids in late anaphase. These data indicate that cytoplasmic dynein is attached to the microtubules in sea urchin mitotic spindles. Considering the sporadic existence and proximity to the microtubules, dynein could belong to the larger granules and crossbridges observed on microtubules by the quick-freeze, deep-etch technique. The data also suggest that dynein and crossbridges between microtubules could be an important part of the machinery of chromosome movement.

THE JOURNAL OF CELL BIOLOGY · VOLUME 101 NOVEMBER 1985 1858–1870

The mitotic apparatus as well as ciliary and flagellar axonemes are typical motile systems composed mainly of microtubules (3, 20, 21, 33). Microtubules are also important cytoskeletal elements in other systems such as axons and chromatophores (15, 16, 37). Although the mechanism of motility based on structural and biochemical studies is relatively well understood in the axonemes (10), it is still ambiguous in the mitotic apparatus.

Several attractive hypotheses have been proposed to account for the mechanism of anaphase chromosome movements, chromosome-to-pole movements (anaphase A) and spindle elongation (anaphase B) (13, 25, 27, 29, 32). Recently, involvement of dynein-like ATPase in these processes has been suggested by physiological and biochemical studies (4, 5, 32). Using the isolated mitotic apparatus or permeabilized PtK1 cell model, chromosomal movement or spindle elongation has been induced by ATP and inhibited by vanadate, erythro-9-(3-[2-hydroxynonyl]) adenine, or antibodies to flagellar dynein (4, 5, 32). In addition, a dynein-like ATPase has been isolated and characterized biochemically from sea urchin egg cytoplasm or mitotic spindles (19, 24, 30, 31, 40). Hisanaga and Sakai (17, 18)[1] have purified cytoplasmic dynein from sea urchin eggs and raised monoclonal antibodies (mAb's)[2] to flagellar dynein that cross-react specifically with cytoplasmic dynein.[1] They have observed that these mAb's stain mitotic spindles of sea urchin eggs by immunofluorescent microscopic studies (18*a*).[1]

Recently, the quick-freeze, deep-etch (QFDE) technique has provided a resolution high enough to demonstrate macromolecular structures and is especially useful for visualizing the three-dimensional architecture of cytoskeletons (12, 14). In the present work, we studied the isolated mitotic apparatus from sea urchin eggs and microtubule proteins isolated from mitotic apparatus by the QFDE technique and by electron microscopic immunocytochemistry using anti-dynein mAb in order to understand the cytoskeletal structure of the mitotic apparatus in molecular detail and to identify its chemical components.

MATERIALS AND METHODS

Isolation of Mitotic Apparatus from Sea Urchin Eggs: Eggs from sea urchin *Pseudocentrotus depressus* and *Hemicentrotus pulcherrimus* were used. Gametes were obtained by injection of 0.5 M KCl into the body cavity. After washing with artificial sea water, the eggs were fertilized. Immediately a large volume of 1 M urea was added and the eggs were passed through a nylon mesh (70 μm) to remove fertilization membranes. They were washed with Ca^{++}-free sea water and cultured until they reached metaphase or anaphase of the first division. Mitotic apparatus was isolated by a method described by Sakai (33) and Endo et al. (6) using 1 M glycerol, 10% dimethyl sulfoxide, 1 mM EGTA, 0.5–1 mM $MgCl_2$, 1% Nonidet P-40, 10 mM PIPES buffer, pH 6.6, containing 1 mM phenylmethylsulfonyl fluoride and 10 μg/ml leupeptin, or by methods described by Salmon (34) using 5 mM EGTA, 0.5 mM $MgCl_2$, 50 mM PIPES, 1% Nonidet P-40 with or without 20% glycerol containing 1 mM phenylmethylsulfonyl fluoride and 10 μg/ml leupeptin.

QFDE Electron Microscopy: Isolated mitotic apparatus was centrifuged at 1,000 *g* for 5 min at room temperature. Some of the pellets were suspended with PEM buffer (10–25 mM PIPES, 1 mM EGTA, and 1 mM $MgCl_2$, pH 6.7) containing 0.1 M K-glutamate, 10 μM taxol. The other pellets were suspended in PEM (0.1 M PIPES) with or without 10 μM taxol. Then the suspension was centrifuged again at 1,000 *g* for 5 min. The pellets were divided into two groups. One was quick frozen directly and the other was fixed with 2% glutaraldehyde in PEM containing 10 μM taxol for 2 h followed by quick freezing after a brief wash with distilled water. Freeze-fracture, deep-etching, and electron microscopy were carried out as described previously (12, 14).

High Salt Extraction: Pellets of isolated mitotic apparatus were divided into two groups. One group was incubated with PEM (0.1 M PIPES) containing 10 μM taxol as a control, and the other group was incubated with PEM (0.1 M PIPES) containing 0.6 M NaCl and 10 μM taxol for 10 min at room temperature. After centrifugation at 1,000 *g* for 5 min, they were resuspended in PEM (0.1 M PIPES) containing 10 μM taxol. Then they were centrifuged again and pellets were quick frozen.

Isolation of Microtubules from Isolated Mitotic Apparatus: Microtubules were isolated from mitotic apparatus using taxol (36, 39). Isolated mitotic apparatus was washed three times with PEM (0.1 M PIPES) by repeating centrifugation and suspension. The resulting pellets were homogenized in 2 vol of PEM (0.1 M PIPES) on ice with a Dounce teflon pestle homogenizer and then incubated for 45 min on ice. The homogenate was centrifuged at 30,000 *g* for 30 min, and the pellet was discarded. The supernate was then centrifuged at 150,000 *g* for 60 min and the pellet again discarded. Taxol and GTP were added to the supernate to get final concentrations of 20 μM (taxol) and 1 mM (GTP), respectively. The supernate was split into two groups. The one was warmed at 37°C for 20 min and the microtubules that were formed were centrifuged at 30,000 *g* for 30 min through a cushion of 10% sucrose in PEM (0.1 M PIPES) containing 10 μM taxol. The other supernate was warmed at 37°C for 15 min and then NaCl was added to 0.6 M. It was incubated at 37°C for 10 min and centrifuged at 30,000 *g* for 30 min through a cushion of 10% sucrose in PEM (0.1 M PIPES) containing 10 μM taxol. The resulting pellets were washed with PEM (0.1 M PIPES) plus 10 μM taxol and processed for SDS PAGE and quick freezing. SDS PAGE (4–10% gradient gel) was carried out according to a method described by Laemmli (23).

Immunocytochemistry: The spindle pellets were washed once with PEM (0.1 M PIPES) containing 0.1 M K glutamate, 1 mM phenylmethylsulfonyl fluoride, and 10 μg/ml leupeptin. They were centrifuged and fixed with 0.1% glutaraldehyde, 1% paraformaldehyde in PEM (0.1 M PIPES) for 1 h. After washing three times with PEM (0.1 M PIPES) containing 0.1 M K-glutamate and 1 M glycerol, they were incubated with culture medium containing a monoclonal antibody (D57) against sea urchin sperm flagellar 21S dynein.[1] As control, a culture medium containing a monoclonal antibody against rat neurofilament 200-kD protein as well as a P3U1 myeloma culture medium were used. They were incubated with culture media diluted two- to fourfold with PEM (0.1 M PIPES) containing 0.1 M K-glutamate and 1 M glycerol for 2 h at room temperature. They were then washed three times with Tris-buffered saline (20 mM Tris buffer, 0.15 M NaCl) containing 0.1% bovine serum albumin (BSA) and incubated with (5 nm) gold-labeled second antibodies (Janssen Pharmaceutica, Belgium) diluted 40-fold with the Tris-buffered saline containing 1% BSA overnight at 4°C. After washing with Tris-buffered saline containing 0.1% BSA, the pellets were fixed with 1% glutaraldehyde in 0.1 M sodium cacodylate buffer for 1 h, followed by postfixation with 1% OsO_4 in the same buffer for 1 h. Sometimes the materials were embedded in agar at this step. They were dehydrated with graded alcohols and embedded in Epon.

Ultrathin sections were cut and observed with a JEOL 1200 EX electron microscope after staining with uranyl acetate and lead citrate.

Quantitation: Four micrographs from different mitotic apparatus were enlarged at 44,000x. The distance between the surface of the microtubules and the center of gold particles was measured by a micrometer. When the gold particles were located on the microtubules the distance was considered as 0. A total of 1,009 gold particles were examined.

Micrographs from isolated mitotic apparatus and microtubules with MAPs polymerized in vitro were enlarged at 190,000–285,000x. The center-to-center space between small granules (buttons) on the microtubule surface and the distance between adjacent stripes on the inner surface of microtubules were measured by a micrometer.

RESULTS

QFDE Electron Microscopy of Isolated Mitotic Apparatus

We have studied the three-dimensional ultrastructure of the mitotic apparatus by the use of the QFDE technique through metaphase to anaphase. Fig. 1 provides a low mag-

[1] Hisanaga, S., T. Tanaka, T. Masaki, H. Sakai, I. Mabuchi, and Y. Hiramoto, manuscript submitted for publication.

[2] *Abbreviations used in this paper:* mAb, monoclonal antibody; MAP, microtubule-associated protein; PEM, 10–25 mM PIPES, 1 mM EGTA, 1mM $MgCl_2$, pH 6.7; QFDE, quick-freeze, deep-etch.

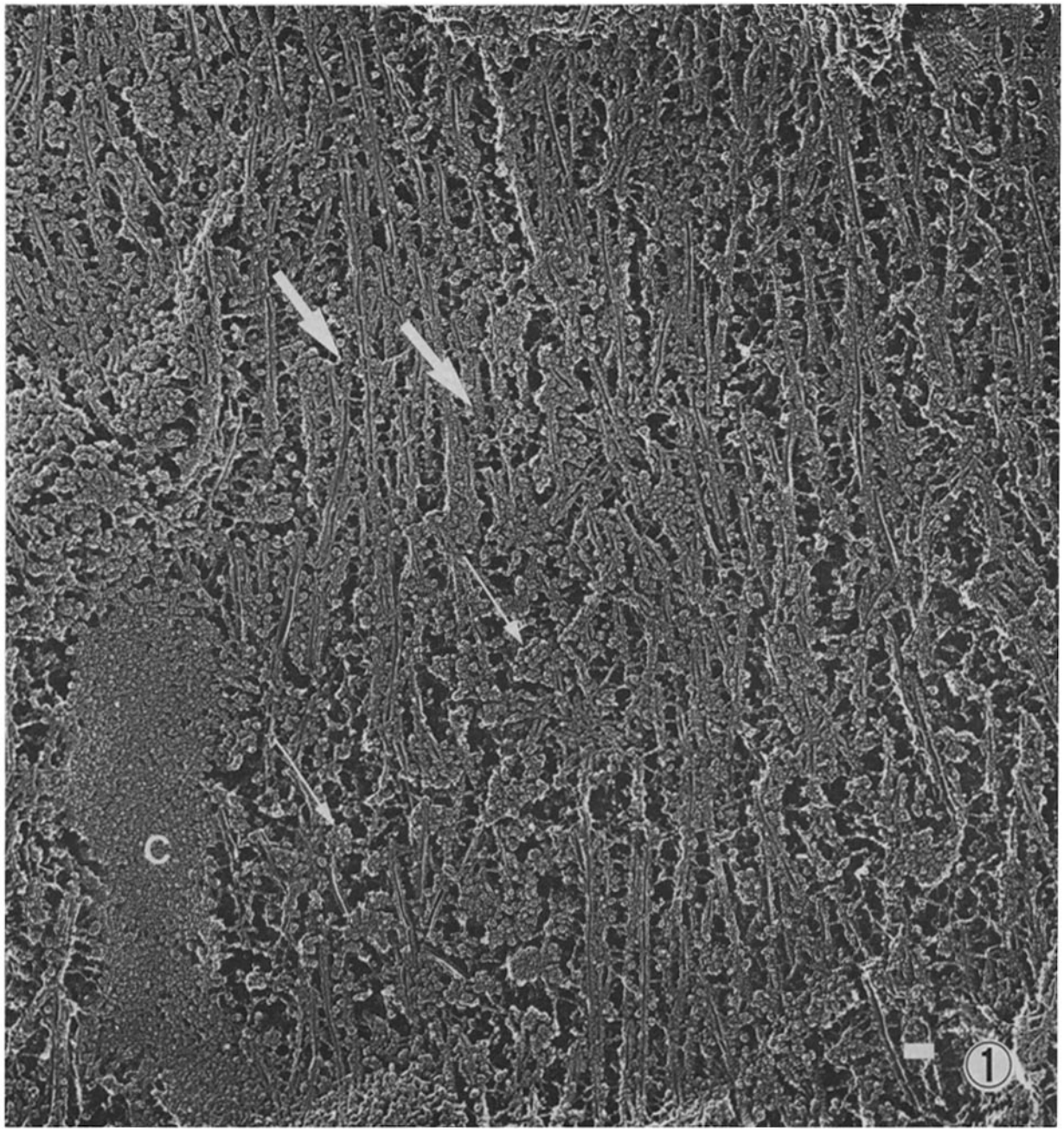

FIGURE 1 A low magnification view of an isolated metaphase mitotic spindle. Parallel arrays of numerous spindle microtubules, a network of crossbridges between microtubules, and clusters of globular substances (long thin arrows) in the network of crossbridges and a chromosome (C) are observed. The surface of microtubules is coated with granular materials (thick arrows). Bar, 0.1 μm. × 50,000.

nification view of an isolated mitotic apparatus. The mitotic apparatus consists of (*a*) chromosomes, (*b*) parallel arrangements of microtubules, (*c*) granular materials associated with microtubules, (*d*) extensive crossbridges between microtubules, and (*e*) clusters of globular substances attached to the crossbridges and microtubules, which probably correspond to the ribosome-like particles described by Salmon and Segall (35). The striking features revealed by the QFDE technique were the extensive crossbridges and granular materials associated with microtubules (see Figs. 1, 2, 4, and 5), which will be described below in more detail. Basically similar results were obtained from both *Pseudocentrotus depressus* and *Hemicentrotus pulcherrimus* by different procedures for obtaining pellets of mitotic apparatus (see Materials and Methods).

The Surface of Spindle Microtubules Is Covered with a Regular Pattern of Small Granules (Microtubule Buttons) and with More Sporadic Larger Granules

Interestingly, the surface of spindle microtubules was covered with at least two kinds of granules, smaller ones and larger ones (see Figs. 1, 2, 4, and 5). The smaller granules took a dome-like shape and looked like buttons. They were hexagonally packed and tended to cover the entire surface of

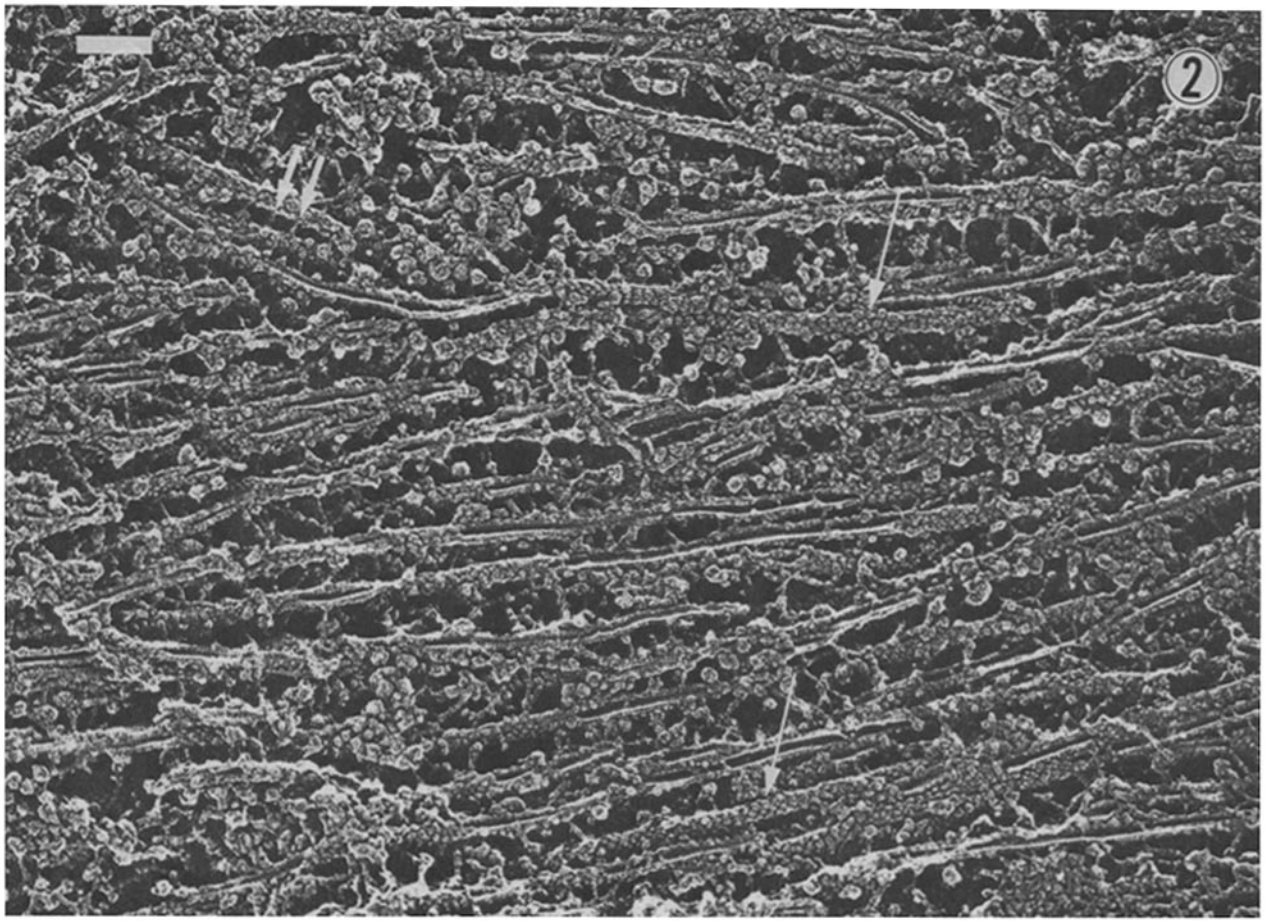

FIGURE 2 This electron micrograph shows extensive crossbridges between spindle microtubules. The crossbridges consist of a short straight type (short arrows) and longer straight or branching type. Clusters of globular substances varying in sizes are attached to the crossbridges. The surface of microtubules was covered by hexagonally packed small granules (long arrows) and occasional larger granules. Bar, 0.1 μm. × 102,000.

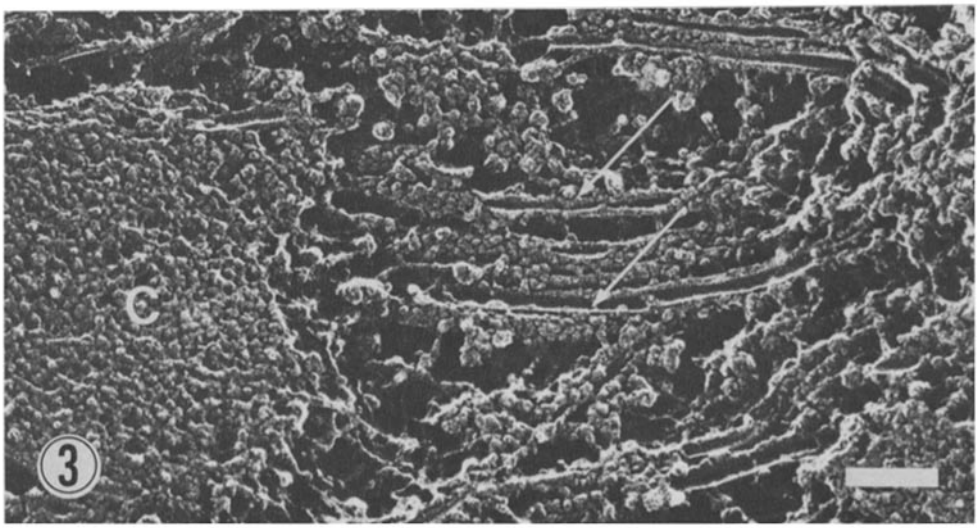

FIGURE 3 Higher magnification view of kinetochore regions. Kinetochore microtubules tended to be arranged close to each other. Short straight side arms were predominantly found between microtubules. The surface of microtubules was covered with granular materials. A network of fine filamentous structure was found between microtubules and chromosomes (C). Arrows indicate microtubules split in half. Bar, 0.1 μm. × 121,000.

spindle microtubules including polar, kinetochore, and astral microtubules (Figs. 2–5). The center-to-center distance between these microtubule buttons arranged side by side and parallel to the long axis of microtubules was 11.8 ± 2.3 nm. That of successive buttons at an angle of 11° (right-handed helix) to the horizontal axis of microtubules was 14.4 ± 1.1 nm (see Fig. 9). The buttons were round in shape and quite uniform in size; they were 7.2 ± 1.1–8.5 ± 1 nm in diameter.

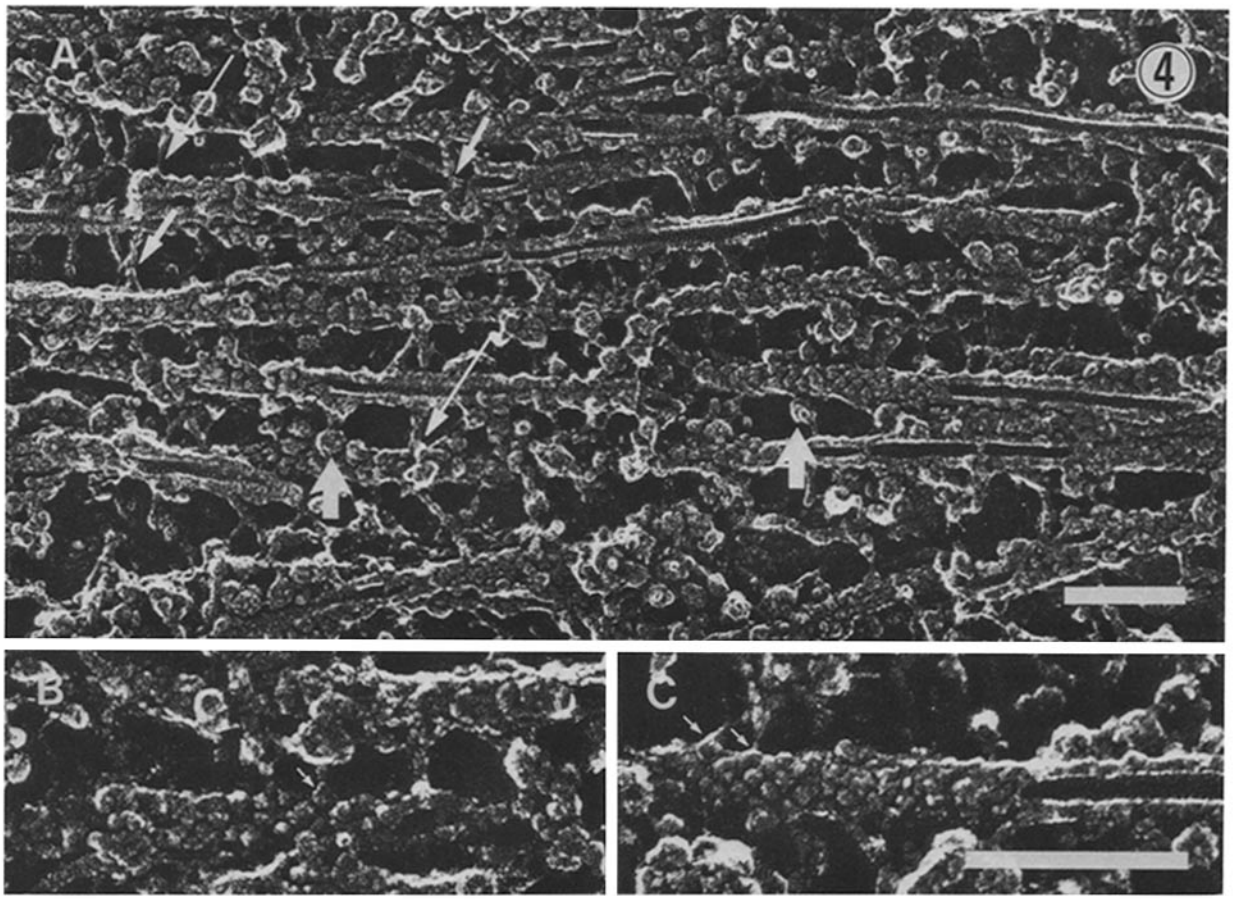

FIGURE 4 A high magnification view of spindle microtubules. The surface of microtubules is decorated by hexagonally packed microtubule buttons and occasional large spherical granules (thick arrows), from which fine tails sometimes extend to adjacent microtubules. Long thin arrows point to straight crossbridges and short arrows indicate branching crossbridges. (*B* and *C*) Higher magnification views showing the relationships between microtubule buttons and crossbridges. Arrows point to small granules where crossbridges terminate. Bars, 0.1 μm. (*A*) × 170,000. (*B* and *C*) × 313,000.

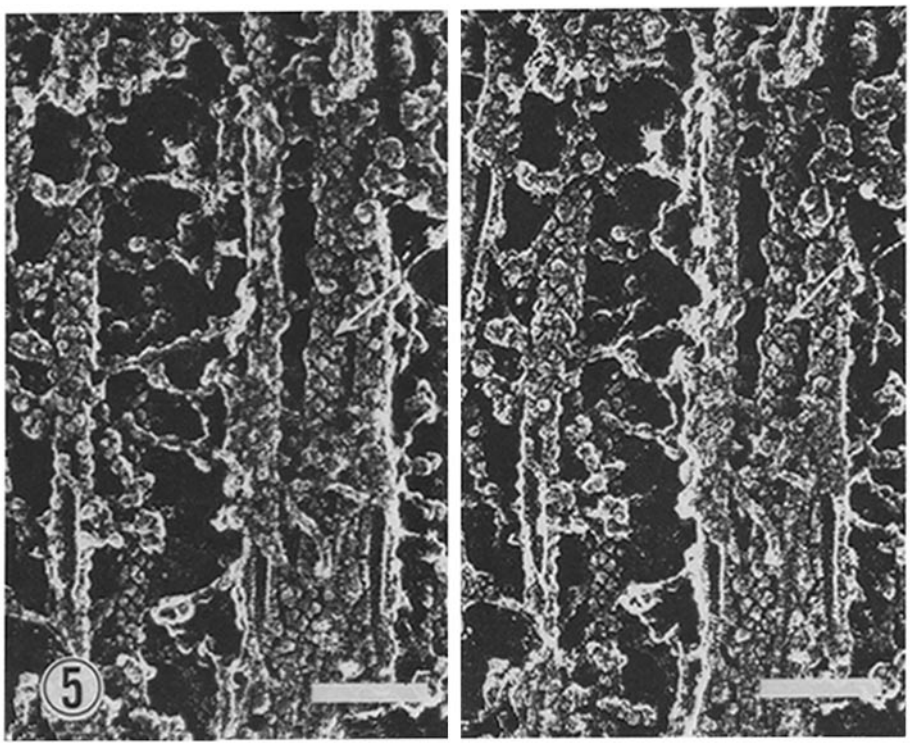

FIGURE 5 A stereo pair of micrographs to show microtubule buttons hexagonally packed on the surface of microtubules. An arrow points to a granule with a central pit. Bar, 0.1 μm. × 154,000.

Occasionally we observed a pit in the center of the buttons (Fig. 5). Crossbridges tended to terminate on these granules (Fig. 4).

Granules of the other type were also associated with microtubules. These granules were larger in size (11–26 nm in diameter) and were mostly spherical but variable in shape (Figs. 1, 2, and 4). Tail-like projections were sometimes observed to connect these granules with adjacent microtubules (Fig. 4). Because of their variability as to size and shape, they may in fact represent different kinds of granules.

Extensive Crossbridges between Spindle Microtubules

Extensive networks of crossbridges were observed between microtubules. They were either a simple straight type or a branching type, and globular substances were also embedded within these networks (Figs. 1, 2, and 4). The shortest straight-type crossbridges between adjacent microtubules were 3–7 nm in diameter and ~20 nm in length (Figs. 1, 2, 4, and 5); a longer straight-type crossbridge (4–9 nm in diameter and 30–40 nm in length) was also found, which was sometimes seen to branch out (Figs. 1, 2, and 4).

Because microtubules of different domains of mitotic spindles such as kinetochore or polar microtubules may participate in chromosomal movement by generating different types of movement such as pole-to-pole elongation or shortening of chromosome-to-pole distance, it was of interest to see whether there was any regional difference in the ultrastructure connecting the microtubules. Although microtubules at the kinetochore region tended to be close to each other so that crossbridges of the short straight type were dominant, extensive crossbridges of various types were found basically between all microtubules including polar and kinetochore microtubules (Figs. 1–4). The polar microtubules in the region between opposing sister chromatids of anaphase mitotic spindles were also connected with a similar type of crossbridge network.

Because isolated mitotic spindles were used in the present study, soluble proteins which were not specific components of spindles can be expected to have been washed away during isolation procedure. Therefore, the observed crossbridges and granular materials should be specific elements of spindles. To circumvent the possibility that salt may cause some artificial structures, we also observed the fixed mitotic apparatus which was frozen after washing with distilled water. Basically, similar crossbridges and globules were observed to be attached to microtubules in these samples as well. This indicated that the crossbridges and granular materials are not caused by mere precipitation of salt (28). We have also tried different procedures to isolate mitotic spindles (see Materials and Methods). Although granules and crossbridges tended to be preserved better in samples processed with solution containing taxol after isolation of mitotic apparatus, basically the structures described here were observed in all samples.

Extraction by High Salt Removed Most Granules and Crossbridges Attached to Microtubules

As one approach for analyzing chemical nature of the structures observed, the mitotic apparatus was treated with high salt (0.6 M NaCl). After this treatment, most granules and crossbridges attached to the surface of microtubules were removed, leaving only a few crossbridges and some clumps of granular materials between the microtubules. Thus the surface of the microtubules looked much clearer after this treatment and arrangement of protofilaments was clearly observable (Fig. 6). This kind of high salt treatment extracts both MAPs and dynein-like ATPase molecules from microtubules (17).

Structure and Components of Microtubules Isolated from Mitotic Apparatus

To clarify the ultrastructure of microtubules in the mitotic apparatus, they were prepared from the isolated mitotic apparatus using taxol. The QFDE technique interestingly revealed that the surface of microtubules was entirely covered with small granules (Fig. 7). These granules were quite uni-

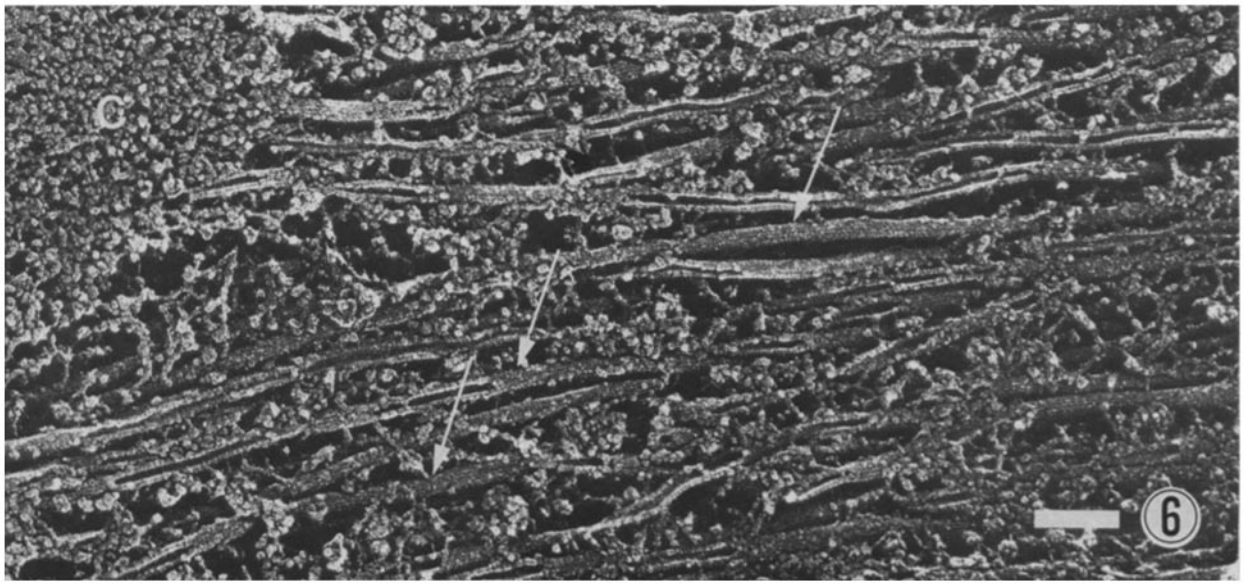

FIGURE 6 Spindle microtubules after extraction with high salt (0.6 M NaCl). This treatment removed most granules and crossbridges attached to the surface of microtubules. The surfaces of microtubules tend to be clear (arrows). Some clumps of granules are left between microtubules. *C*, chromosome. Bar, 0.1 μm. × 122,000.

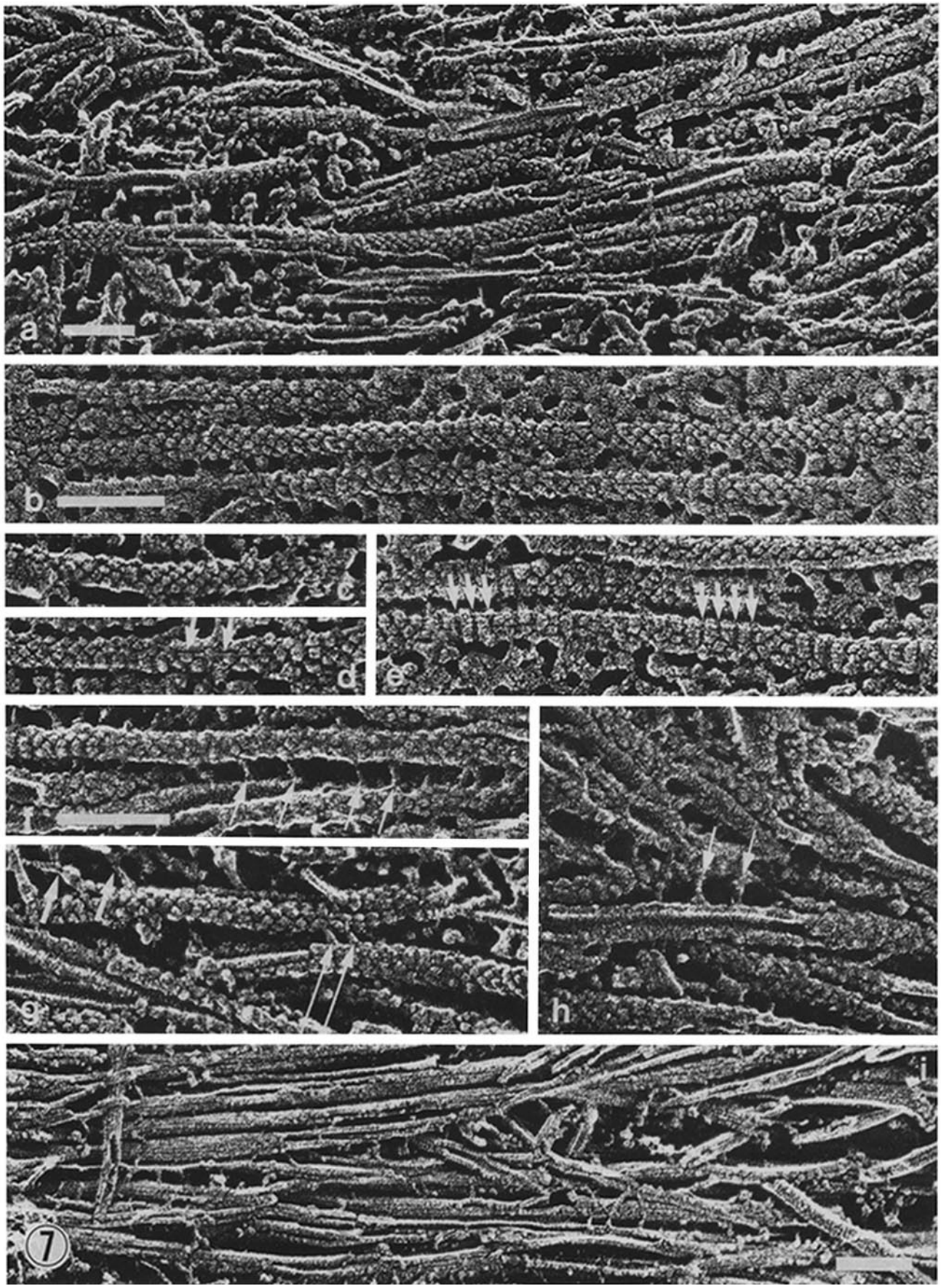
a
b
c
d
e
i
g
h
j
7

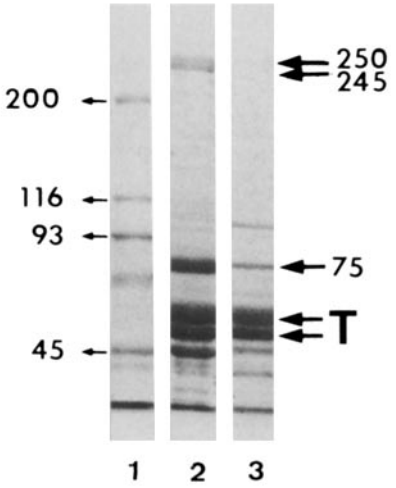

FIGURE 8 Microtubules and MAPs prepared from isolated mitotic apparatus by the taxol/salt method. Lane *1*, molecular marker; lane *2*, pellet of microtubules and MAPs; lane *3*, tubulin-containing pellet after incubation in assembly buffer containing taxol and 0.6 M NaCl. Microtubule pellet prepared from isolated mitotic apparatus by taxol contains a large amount of 75-kD protein and some high molecular weight proteins (250 kD, 245 kD) (lane *2*). After extraction with high salt, the 75-kD protein and high molecular weight proteins were released prominently from the microtubule pellet (lane *3*). A 43-kD protein is probably actin which contaminated in the preparation and is also found in SDS gels of all the previous studies (22, 36, 39). *T*, tubulin.

form in size and hexagonally packed (Fig. 7). They looked just like the microtubule buttons observed on the surface of microtubules in mitotic spindles. The center-to-center distance between buttons side by side parallel to the horizontal axis of microtubules was ~14 nm. The buttons were aligned on a line rising to the right at an angle of 11° to the horizontal axis of microtubules (see Figs. 7 and 9). The characteristic striations observed in the inner luminal walls of microtubules in the same replica were right-handed three-start helices and were separated by 3.6 nm (see Figs. 7.*g* and 9). They were arranged at an angle of about 11° to the horizontal axis of microtubules (Fig. 7*g*). These striations probably reflect the arrangement of tubulin monomers (see Fig. 9). The buttons are 7–8 nm in diameter. We sometimes found hints of boundaries between adjacent protofilaments which buttons overstep (Fig. 7*d*). As shown in Fig. 7*e*, 14 nm stripes were sometimes observed on the microtubule surfaces. The knife probably touched this area and removed some of the granules. The striations form an angle of 11° from the horizontal axis of microtubules.

Besides the small uniform granules, short side arms (<20 nm in length) sometimes cross-linked adjacent microtubules. Longer crossbridges were also associated with microtubules (Fig. 7, *f–h*). These side arms and longer crossbridges respectively resemble the shortest straight-type crossbridges and longer crossbridges between adjacent microtubules observed in mitotic spindles.

The microtubule proteins prepared from isolated mitotic apparatus using taxol were analyzed by SDS gel electrophoresis. The MAPs prepared from mitotic apparatus consisted of mainly 75-kD protein as well as some higher molecular weight proteins (e.g., 245 kD and 250 kD) possibly equivalent to the proteins of similar molecular weight identified by others (22, 36, 39) (Fig. 8). The amount of 75-kD protein relative to tubulin was much higher in this preparation than it was in microtubule proteins isolated from whole eggs (39) (Fig. 8).

Judging from the abundance of microtubule buttons and the relative amount of proteins in the preparation, this structure is probably composed of 75-kD MAP. This conclusion was supported by the high salt extraction experiment. As shown in Fig. 8, the high salt treatment extracted a large amount of 75-kD MAP and high molecular weight MAPs. In these samples, the surfaces of microtubules were mostly clear, lacking the small granules and most of the crossbridges (Fig. 7*i*).

Electron Microscopic Immunocytochemistry Using the mAb to Dynein ATPase

Although the presence of dynein ATPase in mitotic spindles and its participation in chromosomal movement has been proposed previously (4, 5, 18, 24, 30–32, 40), the structural evidence was lacking. We used an mAb (D57) reacting with cytoplasmic dynein to identify dynein ATPase structurally in mitotic spindles. This mAb was raised against sea urchin sperm flagellar 21S dynein. It has been shown that this mAb reacts specifically with sperm flagellar dynein and sea urchin egg dynein by the immunoblotting method.[1] It has also been shown that this mAb stains sperm flagella and the mitotic apparatus of sea urchin egg by immunofluorescence microscopy (18*a*).[1] To make the localization of dynein in mitotic spindles visible at the electron microscopic level, we labeled isolated mitotic spindles by the immunogold technique and observed the samples by thin sectioning. As shown in Fig. 10, immunogold tended to localize close to microtubules, but not to the other structures such as chromosomes or clusters of ribosome-like particles. Most of the gold particles were closely

FIGURE 7 QFDE electron micrographs of microtubules and MAPs prepared from isolated mitotic apparatus by the taxol/salt method. *a* to *h* were taken from the sample of lane *2* and *i* was taken from the sample of lane *3* in Fig. 8. (*a*) A lower magnification view. The surface of microtubules is entirely covered with hexagonally packed microtubule buttons. × 129,000. (*b–e*) High magnification views of microtubules processed by shallow etching. × 200,000. The surfaces of microtubules are just barely exposed from the ice. The hexagonally packed buttons are well observed in *b* and c. In *d*, hints of a boundary between adjacent protofilaments are found (arrows). In e, because the knife sometimes removes some granules, regular ~14-nm stripes aligned at an angle of ~11° relative to the horizontal axis of microtubules were observed (arrows). (*f–h*) Higher magnification views of deep-etched samples to display crossbridges associated with microtubules. × 205,000. In *f*, short straight crossbridges connect adjacent microtubules (arrow). In *g*, some longer crossbridges (long arrows) and short crossbridges are observed. Short crossbridges appear to terminate on the small granules (short arrows). Right-handed helical stripes are found on the inner surface of microtubules. In *h*, short crossbridges (arrows) link adjacent microtubules. (*i*) A low magnification view of microtubules treated with high salt (0.6 M NaCl). Most of the microtubule buttons and crossbridges are removed from the surface of microtubules. × 139,000. Bars, 0.1 μm.

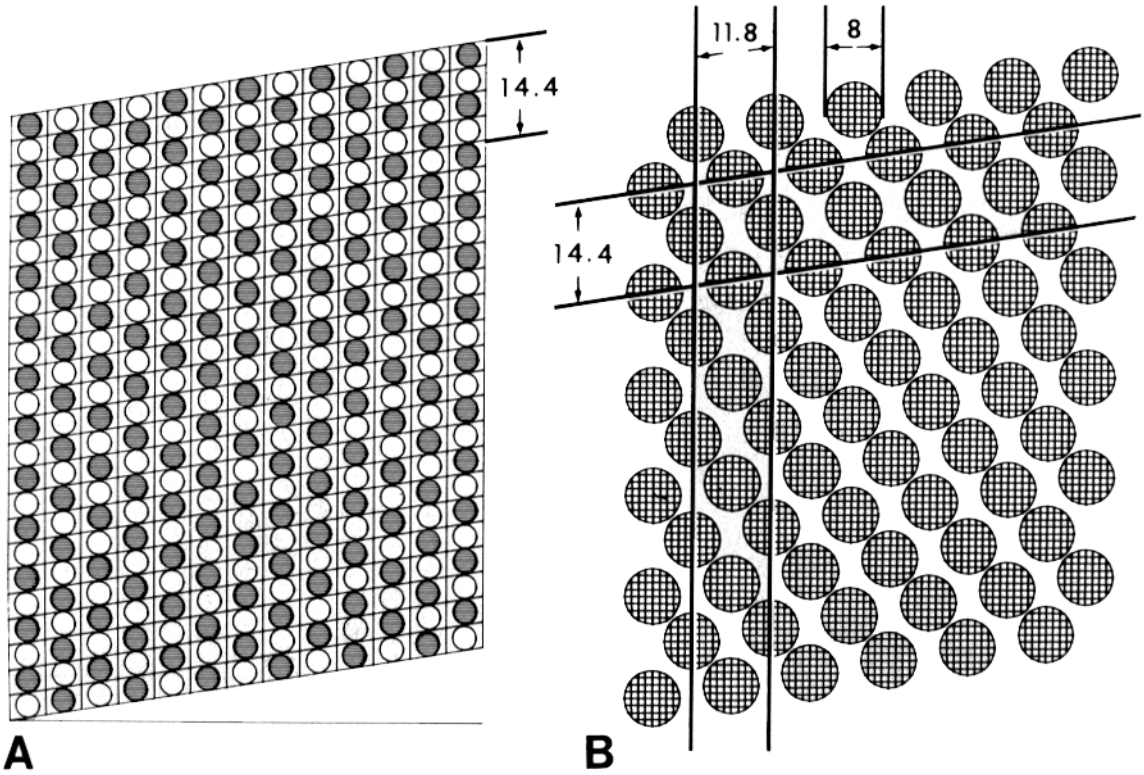

FIGURE 9 Schematic diagram showing the arrangements of tubulin dimers (*A*) and microtubule buttons (*B*) based on the present study. The protofilaments are oriented from top to bottom in this diagram. (*A*) A portion of the microtubule wall "unrolled" to show the packing of tubulin dimers. Arrangement and size of tubulin monomer was determined by the oblique striation on the inner surface of microtubules. The striation was aligned at an angle of 11° relative to the horizontal axis of microtubules. The distance between adjacent stripes was 3.6 nm so that two tubulin dimers probably measure 14.4 nm long along the protofilaments. (*B*) The unrolled helical lattice of microtubule buttons.

associated with the microtubule surface (Figs. 10 and 11). We quantified the association of gold particles and microtubules by measuring the distance between them, as described in Materials and Methods. 76% of the gold particles were located <50 nm away from microtubule surfaces, and 55% were <20 nm away (Fig. 13). These numbers substantiate the close association of dynein molecules and microtubules in mitotic spindles.

Because there has been some controversy as to whether dynein ATPase is involved in pole-to-pole elongation or chromosome-to-pole movement (4), we wanted to establish whether gold particles labeled polar or kinetochore microtubules. In fact, the particles were found not only on the polar microtubules, but also on the kinetochore microtubules in the metaphase and anaphase mitotic apparatus. It is sometimes not easy to identify kinetochore microtubules from single sections. Fig. 10 depicts semi-serial sections of kinetochore microtubules in the early anaphase. Gold particles were seen very close to them. The gold particles were also associated with microtubules in the space between sister chromatids in late anaphase spindles (Fig. 11). In control samples incubated with either a culture medium containing an mAb against rat neurofilament 200-kD protein or P3U1 myeloma culture medium for the first step, immunogold particles were very rarely found in the mitotic apparatus (Fig. 12).

DISCUSSION

The present study has shown for the first time that spindle microtubules were covered by hexagonally packed small round granules (microtubule buttons) quite uniform in size (7–8 nm in diameter) as well as by occasional larger spherical granules (11–26 nm in diameter). The former frequently served as bases for crossbridges, and sidearms sometimes connected the latter with the microtubule surface. The QFDE technique has also revealed extensive crossbridges between spindle microtubules which were composed of both straight and branched types.

After high salt extraction most of the buttons, larger granules and crossbridges associated with microtubules were removed. MAPs isolated from mitotic spindles were composed of mainly 75-kD protein and some high molecular weight proteins (245 kD, 250 kD).

The QFDE technique has demonstrated that microtubules polymerized with MAPs were decorated by hexagonally packed small granules with similar size which resembled the microtubule buttons observed in vivo. Short side arms and some long crossbridges were also identified in microtubules and MAP preparations. These crossbridges look like the short straight crossbridges and long crossbridges observed in vivo. High salt treatment extracted most of 75-kD protein and high molecular weight proteins and removed microtubule buttons and most of the crossbridges from the surface of microtubules. Thus, it was concluded that at least these microtubule buttons and some crossbridges are MAPs and that the microtubule buttons are most probably composed of 75-kD protein. In addition, electron microscopic immunocytochemistry using monoclonal anti-dynein ATPase showed that cytoplasmic dynein molecules exist very close to spindle microtubules. These results suggest that dynein could belong to the larger

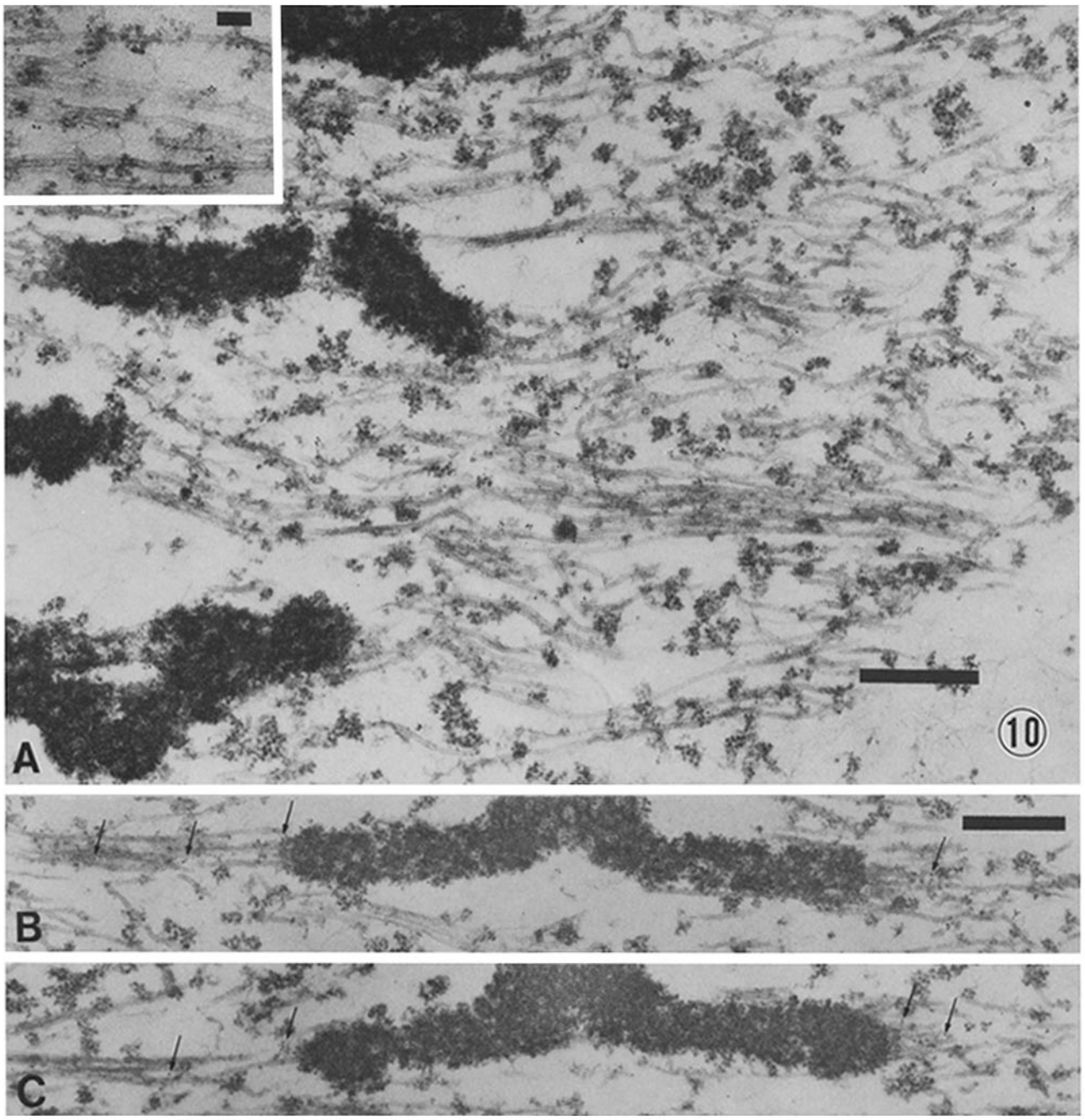

FIGURE 10 (*A*) Electron microscopic immunocytochemistry using anti-dynein ATPase mAb (D57) and gold-labeled anti-mouse IgG. Gold particles (5 nm in diameter) tend to be localized close to the spindle microtubules in the early anaphase. Bar, 0.5 μm; × 38,000. (*Inset*) Higher magnification. Bar, 0.1 μm; × 54,000. (*B* and *C*) Semi-serial sections showing a chromosome and kinetochore microtubules in early anaphase stained with D57. Gold particles are associated with kinetochore microtubules (arrows). Bar, 0.5 μm; × 32,000.

granular material and crossbridges, and that in association with microtubules, dynein may very well play an important role in chromosome movement in the mitotic spindle.

Components of Granular Materials

The microtubule button is a quite unique structure. Fig. 9 displays a schematic drawing of hexagonally packed buttons on the surface of microtubules. On the left side, an arrangement of tubulin monomers on the outer surface of microtubules is shown. Although there is some disagreement as to whether the microtubule surface lattice is the left- or right-handed helix (1, 7, 38), we decided it was the right-handed helix. This is because the data presented here were obtained in replicas in which oblique striations on the inner surface of microtubules displayed the right-handed helix (Fig. 7*g*). The arrangment of the microtubule buttons seems to reflect precisely the helix of the microtubule surface lattice.

The buttons are quite regular in size and hexagonally packed, and they are helically arranged at angle of ~11° relative to the horizontal axis of microtubules (the same angle as that of the helically arranged tubulin molecules according to the oblique striations on the inner surface of microtubules).

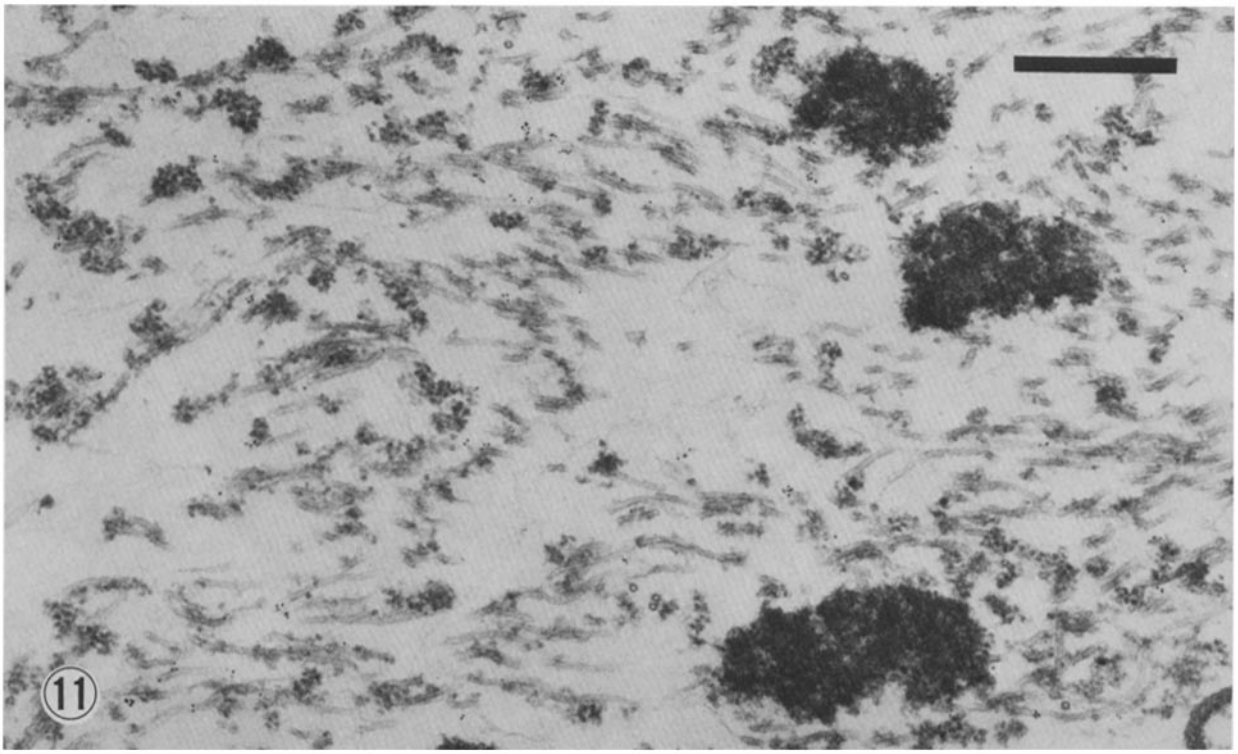

FIGURE 11 A micrograph from late anaphase spindle incubated with anti-dynein mAb (D57). This micrograph shows mainly polar microtubules between sister chromatids (another group of chromosomes on the left side of this picture is not shown). Obviously gold particles are closely associated with polar microtubules at interchromosomal region. Bar, 0.5 μm. × 45,000.

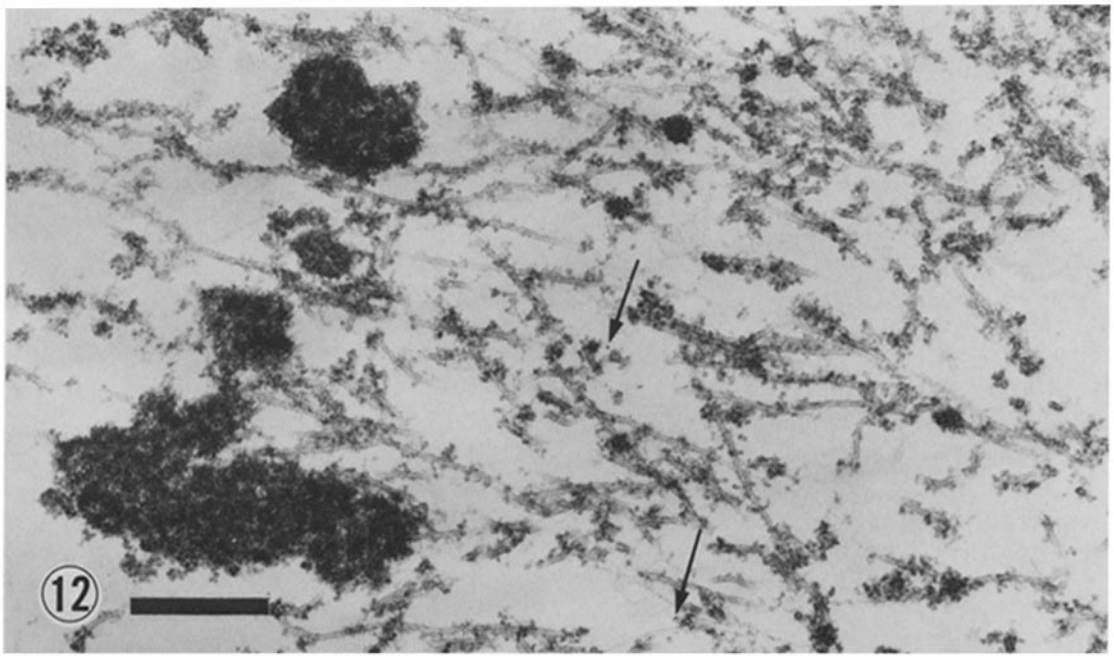

FIGURE 12 An anaphase spindle incubated with control culture medium containing an mAb against neurofilament 200-kD protein at the first step. Immunogold is very rarely found in the spindle (arrows). Bar, 0.5 μm; × 37,000.

The center-to-center distance between granules arranged side by side at an angle of 11° to the horizontal axis of microtubules was 14.4 nm (distance between oblique striations on the inner surface of microtubules is ~3.6 nm), and the granules are 7–8.5 nm in diameter. Therefore, it is reasonable to assume that each granule associates mainly with a single tubulin dimer and tends to span over the immediately adjacent one or two dimers arranged side by side. Thus the arrangement of microtubule buttons possibly reflects the arrangement of tubulin dimers in the microtubules. Further studies are necessary to analyze the molecular interactions between tubulin dimers and microtubule-buttons more accurately; such work is currently underway in this laboratory. Because we found that crossbridges tended to terminate on these granules, the microtubule button may function as a base for crossbridges. This button may also act as a stabilizer of the spindle microtubules.

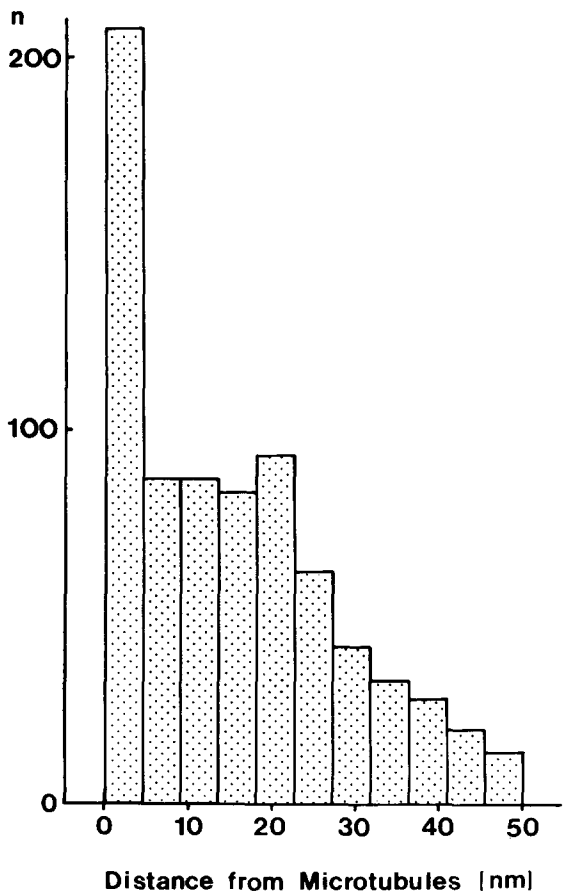

FIGURE 13 A histogram to show the relationship between numbers of gold particles and the distance from microtubules in the mitotic spindles incubated with anti-dynein mAb (D57). 76% of gold particles were <50 nm and ~55% were <20 nm apart from surface of microtubules.

Another type of granule which was associated with microtubules more sporadically was larger in size (11–26 nm in diameter) and sometimes projected short fine tails to the adjacent microtubules. The size of the larger granules fits well into the range of the size of the QFDE image of axonemal dynein composed of globular heads (~17 nm), feet (9 nm), and an arm-like projection (11 nm) (10). Because more than half of the immunogold specific for dynein molecules was observed <20 nm away from the microtubule surface, it is very likely that some of the larger granular attachments and crossbridges consist of cytoplasmic dynein. Our data also coincide well with a recent report showing that dynein-like ATPase isolated from sea urchin egg cross-links microtubules in vitro and that cross-linked microtubules are separated by a gap of 5–20 nm (19). Direct labeling with antibodies using the QFDE technique is necessary to further clarify the molecular structure of a single dynein molecule and is presently in progress in this laboratory.

Components of Crossbridges

QFDE electron microscopy revealed extensive crossbridges between microtubules in mitotic spindles. Several MAPs have been identified in mitotic spindles of sea urchin eggs (36, 39) and other cells (2). Hirokawa et al. (16) have observed an extensive network of crossbridges between microtubules in the axons using the QFDE technique and have proved that high molecular weight MAPs are main components of the crossbridges. Furthermore, isolated MAPs formed cross-linking networks between microtubules composed of simple sidearm types and branching types (16). These crossbridges in vivo and in vitro appear very similar to those seen in the mitotic spindle. Indeed, Vallee and Bloom (39) have observed short and long crossbridges between sea urchin egg microtubules which were polymerized in vitro with MAPs. Salmon and Segall (35) also have described a fuzzy filamentous structure between microtubules in isolated sea urchin mitotic spindle by the thin section method. We found very short straight crossbridges and some longer crossbridges in the quick-frozen microtubules with MAPs. This preparation contained some high molecular weight proteins (245 kD, 250 kD). Therefore, it is reasonable to speculate that MAPs may be another main component of crossbridges found in mitotic spindles. In the axon, the network of crossbridges composed of MAPs ought to change its conformation when organelles pass through it. Similarly, in the mitotic spindle this network of crossbridges can be assumed to be a dynamic structure during chromosome movement.

On the Mechanisms of Chromosome Movement at Anaphase

Chromosome movements at anaphase are composed of distinct sets of events: chromosome-to-pole movement (anaphase A) and spindle elongation (anaphase B).

The elongation of the pole-to-pole distance by the sliding between adjacent polar microtubules, which overlap in a central region (26), has been strongly suggested (25, 26), although the elongation of polar microtubules themselves by assembly of tubulin could be simultaneously taking place (20, 29). The actual molecules involved in the sliding have remained elusive. Recently, Cande (4, 5) has reported that anaphase B is dependent on ATP and is blocked by dynein ATPase inhibitors such as vanadate or erythro-9-(3-[2-hydroxynonyl])adenine, which suggests that dynein may be a motor for the sliding of polar microtubules. We found that cytoplasmic dynein is associated with polar microtubules at metaphase and anaphase and that this dynein also exists on the microtubules between sister chromatids in anaphase. Thus, our data presented structural evidence for the first time that the dynein molecules in fact exist on the polar microtubules, and supports the idea that dynein plays an important role in spindle elongation which is probably induced by the sliding of polar microtubules.

Although it is not known how closely flagellar dynein and cytoplasmic dynein are related, they may have some functional difference. Flagellar dynein cross-links microtubules of the same intrinsic polarity, but polar microtubules originating from opposite spindle poles have opposite polarity (8, 9, 11). However, Warner and Mitchell (41) have shown that dynein cross-links between antiparallel microtubules as well as between parallel microtubules. The molecular mechanism of how dynein molecules generate sliding forces in spindle elongation needs to be further elucidated.

We found that dynein molecules were associated with kinetochore microtubules as well as polar microtubules. Immunofluorescence studies using anti-dynein ATPase antibodies have also shown a positive staining at the kinetochore region.[1] It has been reported that chromosome motion of anaphase A is induced by ATP and is blocked by antiflagellar

dynein serum or vanadate in the isolated mitotic apparatus (32, 33). These studies suggest that dynein-like ATPase also plays a role as a part of the motive force for chromosome movement. However, there is a contradictory report showing that anaphase A does not require exogenous ATP and is unaffected by dynein ATPase inhibitors using a lysed cell model (4). Dynein may play some role in chromosome-to-pole motion although other mechanisms such as disassembly of the kinetochore microtubules are likely to be involved. Physiological studies such as microinjection of antibodies into the fertilized eggs may help clarify this possibility.

We thank Dr. H. Sakai, Mr. T. Tanaka, and Dr. T. Masaki for their valuable suggestions and discussions. We also thank Dr. Y. Hiramoto for the use of his laboratory, Ms. Y. Kawasaki for her technical assistance, and Mr. Y. Fukuda for his photographic work. The authors also wish to thank the editor and reviewers for their helpful advice.

This work is supported by a Grant-in-Aid for Scientific Research from the Japanese Ministry of Education, Science, and Culture and a grant from the Muscular Dystrophy Association of America to N. Hirokawa.

Received for publication 11 March 1985, and in revised form 26 June 1985.

REFERENCES

1. Amos, L. A., and A. Klug. 1974. Arrangement of subunits in flagellar microtubules. *J. Cell Sci.* 14:523–549.
2. Bloom, G. S., F. C. Luca, and R. B. Vallee. 1984. Widespread cellular distribution of MAP-1A in the mitotic spindle and on interphase microtubules. *J. Cell Biol.* 98:331–340.
3. Brinkley, B. R., and J. Cartwright. 1971. Ultrastructural analysis of mitotic spindle elongation in mammalian cells in vitro. *J. Cell Biol.* 50:416–431.
4. Cande, W. Z. 1982. Nucleotide requirements for anaphase chromosome movements in permeabilized mitotic cell: anaphase B but not anaphase A requires ATP. *Cell.* 28:15–22.
5. Cande, W. Z. 1982. Inhibition of spindle elongation in permeabilized cells by erythro 9[3-(2-hydroxynonyl)] adenine. *Nature (Lond.).* 295:700–701.
6. Endo, S., M. Toriyama, and H. Sakai. 1983. The mitotic apparatus with unusually many microtubules from sea urchin eggs treated by hexyleneglycol. *Dev. Growth & Differ.* 25:307–314.
7. Erickson, H. P. 1974. Microtubule surface lattice and subunit structure and observations on reassembly. *J. Cell Biol.* 60:153–167.
8. Euteneuer, U., and J. R. McIntosh. 1981. Polarity of some motility-related microtubules. *Proc. Natl. Acad. Sci. USA.* 78:372–376.
9. Euteneuer, U., and J. R. McIntosh. 1981. Structural polarity of kinetochore microtubules in PtK1 cells. *J. Cell Biol.* 89:338–345.
10. Goodenough, U. W., and J. E. Heuser. 1982. Substructure of the outer dynein arm. *J. Cell Biol.* 95:798–815.
11. Haimo, L. T., and B. R. Telzer. 1981. Dynein–microtubules interaction: ATP-sensitive dynein-binding and the structural polarity of mitotic microtubules. *Cold Spring Harbor Symp. Quant. Biol.* 46:207–217.
12. Heuser, J. E., and S. R. Salpeter. 1979. Organization of acetylcholine receptors in quick-frozen, deep-etched, and rotary-replicated *Torpedo* postsynaptic membrane. *J. Cell Biol.* 82:150–173.
13. Hiramoto, Y., and Y. Shoji. 1982. Localization of the motive force for chromosome movement in sand dollar eggs. *Cell Differ.* 11:349–351.
14. Hirokawa, N., and J. E. Heuser. 1981. Quick-freeze, deep-etch visualizations of intestinal epithelial cells. *J. Cell Biol.* 91:399–409.
15. Hirokawa, N. 1982. Cross-linker system between neurofilaments, microtubules, and membrane organelles in frog axons revealed by the quick-freeze, deep-etching method. *J. Cell Biol.* 94:129–142.
16. Hirokawa, N., G. S. Bloom, and R. B. Vallee. 1985. Cytoskeletal architecture and immunocytochemical localization of microtubule-associated proteins in regions of axons associated with rapid axonal transport: the β,β'iminodipropionitrile–intoxicated axon as a model system. *J. Cell Biol.* 101:227–239.
17. Hisanaga, S., and H. Sakai. 1980. Cytoplasmic dynein of the sea urchin egg. I. Partial purification and characterization. *Dev. Growth & Differ.* 22:373–384.
18. Hisanaga, S., and H. Sakai. 1983. Cytoplasmic dynein of the sea urchin egg. II. Purification, characterization and interactions with microtubules and Ca^{++}-calmodulin. *J. Biochem.* 93:87–98.
18a. Hisanaga, S., and H. Sakai. 1985. Cytoplasmic dynein and mitotic spindle. *Cell Motility.* 5:167–168. (Abstr.)
19. Hollenbeck, P. J., F. Suprynowicz and W. Z. Cande. 1984. Cytoplasmic dynein-like ATPase cross-links microtubules in an ATP-sensitive manner. *J. Cell Biol.* 99:1251–1258.
20. Inoué, S. 1981. Cell division and the mitotic spindle. *J. Cell Biol.* 91:131–147.
21. Inoué, S., and H. Sato. 1967. Cell motility by labile association of molecules: the nature of mitotic spindle fibers and their role in chromosomal movement. *J. Gen. Physiol.* 50:259–292.
22. Keller, T. C. S., III, and L. I. Rebhun. 1982. *Strongylocentrotus purpuratus* spindle tubulin. I. Characteristics of its polymerization and depolymerization in vitro. *J. Cell Biol.* 93:788–796.
23. Laemmli, U. K. 1970. Cleavage of structural protein during assembly of the head of bacteriophage T4. *Nature (Lond.).* 227:680–685.
24. Mazia, D., R. R. Chaffee, and R. M. Iverson. 1961. Adenosine triphosphatase in the mitotic apparatus. *Proc. Natl. Acad. Sci. USA.* 47:788–790.
25. McDonald, K., J. D. Pickett-Heaps, J. R. McIntosh, and D. H. Tippit. 1977. On the mechanism of anaphase spindle elongation in Daitoma Vulgare. *J. Cell Biol.* 74:377–388.
26. McDonald, K., M. K. Edwards, and J. R. McIntosh. 1979. Cross-sectional structure of the central mitotic spindle of Diatoma Vulgare. *J. Cell Biol.* 83:443–461.
27. McIntosh, J. R., P. K. Hepler, and D. G. van Wie. 1969. Model for mitosis. *Nature (Lond.).* 224:659–663.
28. Miller, K. R., C. S. Precott, T. L. Jacobs, and N. L. Lassignal. 1983. Artifacts associated with quick-freezing and freeze drying. *J. Ultrastruct. Res.* 82:123–133.
29. Pickett-Heaps, J. D., D. H. Tippit, and K. R. Porter. 1982. Rethinking mitosis. *Cell.* 29:729–744.
30. Pratt, M. M. 1980. The identification of a dynein ATPase in unfertilized sea urchin eggs. *Dev. Biol.* 74:364–378.
31. Pratt, M. M., T. Otter, and E. D. Salmon. 1980. Dynein-like Mg-ATPase in mitotic spindles isolated from sea urchin embryos (*Strongylocentrotus droebachiensis*). *J. Cell Biol.* 86:738–745.
32. Sakai, H., I. Mabuchi, S. Shimoda, R. Kuriyama, K. Ogawa, and H. Mohri. 1976. Induction of chromosome motion in the glycerol isolated mitotic apparatus: nucleotide specificity and effects of anti-dynein and -myosin sera on the motion. *Dev. Growth & Differ.* 18:211–219.
33. Sakai, H. 1978. The isolated mitotic apparatus and chromosome motion. *Int. Rev. Cytol.* 55:23–48.
34. Salmon, E. D. 1982. Mitotic spindles isolated from sea urchin eggs with EGTA lysis buffer. *Methods Cell Biol.* 25:69–105.
35. Salmon, E. D., and R. R. Segall. 1980. Calcium-labile mitotic spindles isolated from sea urchin eggs (*Lytechinus variegatus*). *J. Cell Biol.* 86:355–365.
36. Scholey, J. M., B. Neighbors, J. R. McIntosh, and E. D. Salmon. 1984. Isolation of microtubules and a dynein-like MgATPase from unfertilized sea urchin eggs. *J. Biol. Chem.* 259:6516–6525.
37. Schliwa, M. 1984. Mechanisms of intracellular organelle transport. *In* Cell and Muscle Motility. S. J. W. Shany, editor. Plenum Publishing Corp. New York. 1–82.
38. Shultheiss, R., and E. Mandelkow. 1983. Three-dimensional reconstruction of tubulin sheets and re-investigation of microtubules surface lattice. *J. Mol. Biol.* 170:471–496.
39. Vallee, R. B., and G. S. Bloom. 1983. Isolation of sea urchin egg microtubules with taxol and identification of mitotic spindle microtubule-associated proteins with monoclonal antibodies. *Proc. Natl. Acad. Sci. USA.* 80:6259–6263.
40. Weisenberg, R., and E. W. Taylor. 1968. Studies on ATPase activity of sea urchin eggs and the isolated mitotic apparatus. *Exp. Cell Res.* 53:372–384.
41. Warner, F. D., and D. R. Mitchell. 1981. Polarity of dynein-microtubule interactions in vitro: cross-bridging between parallel and antiparallel microtubules. *J. Cell Biol.* 89:35–44.